Reflection and diffraction at the end of a cylindrical dielectric nanowire: Exact analytical solution

V. G. Bordo*

A.M. Prokhorov General Physics Institute, Russian Academy of Sciences, 119991 Moscow, Russia

(Received 23 April 2008; revised manuscript received 29 July 2008; published 25 August 2008)

The rigorous theory of reflection and diffraction at the end of a semi-infinite dielectric circular cylinder is developed. An exact solution of this problem is found by the use of fictitious electric and magnetic current sheets located at the end of the cylinder. The solution has the form of the Fourier integral along the integration path in the complex plane of propagation constants. The theory assumes an arbitrary ratio between the cylinder radius and the wavelength and hence it can be used for the description of the nanowire optical properties. The case when the incident wave is a transverse magnetic (TM)/ transverse electric (TE) waveguide mode is analyzed in detail. It is found that such a mode is completely converted into TE/TM-polarized field on reflection from the nanowire facet. It is shown that the corresponding angular diffraction pattern forms a cone which is specific for a given waveguide mode. The obtained results can be used for the determination of the threshold gain and quality factor as well as Fabry-Pérot modes of a nanolaser.

DOI: 10.1103/PhysRevB.78.085318 PACS number(s): 78.67.−n, 42.25.Fx, 81.07.−b

I. INTRODUCTION

Recently, significant progress has been made in fabrication and investigation of submicron-sized optical fibers which are known as nanowires or nanofibers. They can be grown from either inorganic[1–5] or organic[6–8] semiconductor materials and can be obtained by means of drawing from silica.[9] It has been demonstrated that such structures possess promising waveguiding[9–12] and photoluminescence[2,13] properties and can act as a nanolaser.[3–5,11,14–16] The optical measurements with nanofibers include registration of the emitted or scattered light angular distributions in both far-field and near-field microscopy.[17–20] On the other hand, nanowires themselves can be used as optical probes in a novel form of subwavelength microscopy.[21]

Despite progress in experimental techniques, the lack of theory which could describe the nanowire optical response adequately prevents from fundamental understanding of experimental results. The first theoretical model which has been used to treat the interaction between a nanowire and a light beam dates back to Lord Rayleight.[22] It assumes that a nanowire is a circular dielectric cylinder of infinite length. One can modify this model to account for a reflecting substrate,[23] but the restriction imposed on the nanowire length still remains. Such a model does not allow one to describe effects at the nanowire ends, i.e., reflection and diffraction of light. Reflections at the nanowire facets, however, play a key role in lasing and the reflection coefficient determines the threshold gain and quality factor. Besides that, the phase of the reflection coefficient dictates the Fabry-Pérot modes in a nanolaser resonator. The estimates based on the Fresnel formula are obviously inadequate when the nanowire diameter is comparable with or less than the light wavelength.

Although the reflection and diffraction of waveguide modes in a nanowire can be calculated numerically using the finite-difference time-domain method,[24,25] such an approach does not allow comprehensive analysis of the problem. On the other hand, an exact solution, if available, can provide a test for numerical calculations. In the present paper we find an exact solution for the electromagnetic field when a waveguide mode propagates toward the nanowire end. We obtain an analytical expression for the reflection coefficient as well as for the coefficients of transformation of the incident wave into the other waveguide modes. We find also the angular distribution of the diffracted electromagnetic field in the medium surrounding the nanowire.

It should be noted that the diffraction problems allow exact rigorous solutions in closed form only in some special cases. The larger part of them has been solved for metallic (perfectly conducting) objects. They include diffraction by a wedge (and by a semi-infinite plane, in particular), by a slit or by a circular aperture in an infinite plane and the complimentary problems of diffraction by an infinite ribbon or by a circular disk, respectively. A comprehensive overview of those works is given in Ref. 26. Another class of problems deals with diffraction at the open end of an empty semi-infinite waveguide with perfectly conducting walls, either plane or cylindrical.[27] For dielectric obstacles, there are well-known solutions obtained for an infinite circular cylinder and a sphere.[22] An exact rigorous solution has been found also for an arbitrary dielectric spheroid, although it requires much computational efforts.[28] We thus demonstrate in this paper that diffraction at the end of a dielectric cylinder is among these few problems. Let us note that the solutions obtained for particles of a simple shape can be used to simulate light scattering from micro- and nanostructures[29] as well as to get insight into the tip-sample interaction in scanning near-field optical microscopy.[30,31]

The paper is organized as follows: In Sec. II we describe the theoretical model which is used in the paper. We introduce the fictitious electric and magnetic current sheets which simulate the electromagnetic field diffracted at the nanowire end. Sections III and IV deal with general theory of reflection and diffraction at the nanowire end, respectively. These results are applied for the particular case of symmetric incident waveguide modes in Sec. V. The main results are summarized in Sec. VI.

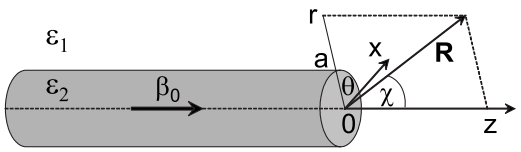

FIG. 1. Geometry of the problem.

II. THEORETICAL MODEL

A. Hertz vectors

We shall model a nanowire by a semi-infinite dielectric cylinder of radius a with the dielectric function ϵ_2 surrounded by medium with the dielectric function ϵ_1 ($\epsilon_2 > \epsilon_1$). Let the z axis of the cylindrical coordinate system (r, θ, z) be directed along the nanowire axis; the nanowire extends toward negative z values and is terminated at $z=0$ (Fig. 1). Assuming that a waveguide mode having the frequency ω propagates from $z=-\infty$ toward the nanowire end, we shall calculate the electromagnetic field both reflected from the nanowire facet and scattered into surrounding medium.

We shall describe the electromagnetic fields in terms of the electric and magnetic Hertz vectors, $\mathbf{\Pi}^e$ and $\mathbf{\Pi}^m$, which correspond to the e-type [or transverse magnetic (TM)] and m-type [or transverse electric (TE)] waves, respectively.[32] Then, implying that all field vectors have the temporal dependence given by $\exp(-i\omega t)$, the electric and magnetic field amplitudes can be found as follows (in Gaussian units):

$$\mathbf{E} = \nabla(\nabla \cdot \mathbf{\Pi}^e) + k_j^2 \mathbf{\Pi}^e + i\frac{\omega}{c} \nabla \times \mathbf{\Pi}^m, \tag{1}$$

$$\mathbf{H} = \nabla(\nabla \cdot \mathbf{\Pi}^m) + k_j^2 \mathbf{\Pi}^m - i\epsilon_j \frac{\omega}{c} \nabla \times \mathbf{\Pi}^e \tag{2}$$

with c as the speed of light in vacuum and

$$k_j = \frac{\omega}{c}\sqrt{\epsilon_j} \tag{3}$$

as the modulus of the wave vector of light outside the nanowire ($j=1$) or inside it ($j=2$).

The incident waveguide mode is defined for an infinite cylinder and is described by the Hertz vectors $\mathbf{\Pi}_j^{(i)e}$ and $\mathbf{\Pi}_j^{(i)m}$. Due to the cylindrical symmetry of the problem these vectors only have a z component given by the equations[33]

$$\Pi_{jz}^{(i)e}(r, \theta, z) = \frac{a_{j0}}{q_{j0}^2} Z_n(q_{j0} r) e^{-in\theta} e^{i\beta_0 z} \tag{4}$$

and

$$\Pi_{jz}^{(i)m}(r, \theta, z) = \frac{b_{j0}}{q_{j0}^2} Z_n(q_{j0} r) e^{-in\theta} e^{i\beta_0 z}. \tag{5}$$

Here $Z_n(\rho)$ is a cylindrical function defined by the condition

$$Z_n(q_j r) = \begin{cases} J_n(q_2 r) & \text{if } r < a \\ H_n^{(1)}(q_1 r) & \text{if } r > a, \end{cases} \tag{6}$$

with J_n and $H_n^{(1)}$ as the Bessel function of the first kind and the Hankel function of the first kind, respectively, β_0 is the propagation constant of the incident wave, n is an integer, and

$$q_{j0} = \sqrt{k_j^2 - \beta_0^2}. \tag{7}$$

The corresponding field amplitudes obtained with the use of Eqs. (1) and (2) are given in Appendix A The coefficients a_{10}, a_{20}, b_{10}, and b_{20} in Eqs. (4) and (5) are chosen so that the tangential field components would be continuous across the boundary $r=a$. For the purpose of definition of the reflection coefficient, we shall introduce also the incident wave amplitude as follows:

$$\psi_j^{(i)} \equiv \Pi_{jz}^{(i)e} + \Pi_{jz}^{(i)m}. \tag{8}$$

B. Fictitious current sheets

Consider the boundary conditions for the field components which have to be satisfied at $z=0$. Let $\mathbf{E}'$ and $\mathbf{H}'$ be the electric and magnetic fields "reflected" from the nanowire facet into the half-space $z<0$ whereas $\mathbf{E}''$ and $\mathbf{H}''$ be the ones "transmitted" into the half-space $z>0$. Then these fields obey the following equations at $z=0$:

$$\mathbf{E}_t'' - \mathbf{E}_t' = \mathbf{E}_t^{(i)}, \tag{9}$$

$$\mathbf{H}_t'' - \mathbf{H}_t' = \mathbf{H}_t^{(i)}, \tag{10}$$

where the subscript t denotes the vector components tangential to the plane $z=0$. Following Schelkunoff,[34] consider now the fields $\bar{\mathbf{E}}$ and $\bar{\mathbf{H}}$ composed of $\mathbf{E}'$ and $\mathbf{H}'$ at $z<0$ and of $\mathbf{E}''$ and $\mathbf{H}''$ at $z>0$. Then, according to Eqs. (9) and (10), one can imagine the fields $\bar{\mathbf{E}}$ and $\bar{\mathbf{H}}$ as being induced by the fictitious electric and magnetic current sheets located at $z=0$ with the surface current densities

$$\mathbf{K}^e = \frac{c}{4\pi} \mathbf{H}_t^{(i)} \tag{11}$$

and

$$\mathbf{K}^m = -\frac{c}{4\pi} \mathbf{E}_t^{(i)}, \tag{12}$$

respectively. The corresponding Hertz vectors either in the nanowire interior ($j=2$) or in its exterior ($j=1$) can be found as the solutions of inhomogeneous wave equations with the sources determined by Eqs. (11) and (12). They have the following form:[32]

$$\mathbf{\Pi}_j^e(\mathbf{R}) = \frac{i}{\epsilon_j \omega} \int_{S_j} \mathbf{K}^e(\mathbf{R}') \frac{e^{ik_j|\mathbf{R}-\mathbf{R}'|}}{|\mathbf{R}-\mathbf{R}'|} d\mathbf{R}', \tag{13}$$

$$\mathbf{\Pi}_j^m(\mathbf{R}) = \frac{i}{\omega} \int_{S_j} \mathbf{K}^m(\mathbf{R}') \frac{e^{ik_j|\mathbf{R}-\mathbf{R}'|}}{|\mathbf{R}-\mathbf{R}'|} d\mathbf{R}', \tag{14}$$

where it is assumed that the currents $\mathbf{K}^e$ and $\mathbf{K}^m$ are taken in the rectangular coordinates (x,y,z). Here the radius-vector $\mathbf{R}'$ runs over the surface S_j in the plane $z'=0$ (plane S). For $z<0$, S_2 is the nanowire facet $(r\leq a)$ and $S_1=S-S_2$; for $z>0$, the surface S_j coincides with S.

The distance between the observation point $\mathbf{R}$ and the elementary current located at $\mathbf{R}'$ can be written in the cylindrical coordinates as

$$|\mathbf{R}-\mathbf{R}'|=\sqrt{d^2+z^2}, \tag{15}$$

where

$$d=\sqrt{r^2+r'^2-2rr'\cos(\theta-\theta')}. \tag{16}$$

Using the identity[35]

$$\frac{e^{ik_j\sqrt{d^2+z^2}}}{\sqrt{d^2+z^2}}=\frac{i}{2}\int_{-\infty}^{\infty}H_0^{(1)}(q_jd)e^{i\beta z}d\beta \tag{17}$$

and the theorem of addition for the cylindrical functions,

$$H_0^{(1)}(q_jd)=\sum_{s=-\infty}^{\infty}J_s(q_jr_<)H_s^{(1)}(q_jr_>)e^{-is(\theta-\theta')}, \tag{18}$$

with

$$q_j=\sqrt{k_j^2-\beta^2},\quad 0\leq \mathrm{Arg}(q_j)<\pi, \tag{19}$$

and $r_<=\min(r,r')$, $r_>=\max(r,r')$, one can express quantities (13) and (14) in terms of the series of the Bessel and Hankel functions.

The fictitious surface currents being written in the cylindrical coordinates acquire the form

$$\mathbf{K}^\sigma(r,\theta)=[\kappa_r^\sigma(r)\mathbf{e}_r+\kappa_\theta^\sigma(r)\mathbf{e}_\theta]e^{-in\theta}, \tag{20}$$

where the superscript σ denotes either electric $(\sigma=e)$ or magnetic $(\sigma=m)$ current, $\mathbf{e}_r$ and $\mathbf{e}_\theta$ are the unit vectors of the coordinate system and the components κ_r^σ and κ_θ^σ are given in Appendix B. Substituting Eq. (20) in Eqs. (13) and (14) and carrying out the integration over θ' with the use of relations (17) and (18) one obtains the Hertz vectors in the form of the Fourier integrals

$$\mathbf{\Pi}_j^\sigma(r,\theta,z)=\frac{1}{2\pi}\int_{-\infty}^{\infty}\tilde{\mathbf{\Pi}}_j^\sigma(r,\theta;\beta)e^{i\beta z}d\beta, \tag{21}$$

with

$$\tilde{\mathbf{\Pi}}_j^\sigma(r,\theta;\beta)=-\frac{\pi^2}{\tau_\sigma\omega}e^{-in\theta}\int_{L_j}[\mathbf{p}_-^\sigma(r')J_{n-1}(q_jr_<)H_{n-1}^{(1)}(q_jr_>)+\mathbf{p}_+^\sigma(r')J_{n+1}(q_jr_<)H_{n+1}^{(1)}(q_jr_>)]r'dr', \tag{22}$$

where $\tau_e=\epsilon_j$, $\tau_m=1$,

$$L_j=\begin{cases}[a,\infty) & \text{if } j=1\\ [0,a] & \text{if } j=2,\end{cases} \tag{23}$$

for $z<0$, $L_1=[0,\infty)$ for $z>0$, and we have introduced the functions

$$\mathbf{p}_\pm^\sigma(r)=[\kappa_r^\sigma(r)\mp i\kappa_\theta^\sigma(r)](\mathbf{e}_r\pm i\mathbf{e}_\theta). \tag{24}$$

The electromagnetic field amplitudes dictated by the Hertz vectors [Eq. (21)] have the form of the Fourier integral as well. The corresponding Fourier-transformed amplitudes for $z<0$ are given in Appendix C.

The following consideration depends on whether one considers the field reflected from the nanowire end or that diffracted into surrounding medium. We shall therefore discuss these cases separately.

III. REFLECTION OF A WAVEGUIDE MODE

Although the Hertz vectors given by Eqs. (13) and (14) satisfy the necessary boundary conditions at $z=0$ they do not provide, however, continuity of tangential field components at the nanowire surface $r=a$ at $z<0$. To fulfill this requirement, we shall add to $\mathbf{\Pi}_j^e$ and $\mathbf{\Pi}_j^m$ a solution of the homogeneous wave equation

$$\Delta\Pi_{jz}^\sigma+k_j^2\Pi_{jz}^\sigma=0 \tag{25}$$

and we shall impose the boundary conditions onto the total electromagnetic field.

We shall seek the general solution of Eq. (25) in the form of the Fourier integral [see Eq. (21)]. Then the quantities $\tilde{\mathbf{\Pi}}_{jz}^\sigma(r,\theta;\beta)e^{i\beta z}$ satisfy the wave equation in the cylindrical coordinates and can be found therefore as follows:

$$\tilde{\mathbf{\Pi}}_{jz}^e(r,\theta;\beta)=\frac{1}{q_j^2}\sum_{m=-\infty}^{\infty}a_{jm}(\beta)Z_m(q_jr)e^{-im\theta}, \tag{26}$$

$$\tilde{\mathbf{\Pi}}_{jz}^m(r,\theta;\beta)=\frac{1}{q_j^2}\sum_{m=-\infty}^{\infty}b_{jm}(\beta)Z_m(q_jr)e^{-im\theta}, \tag{27}$$

where $0\leq\mathrm{Arg}(q_j)<\pi$ and the functions $Z_m(\rho)$ are given by Eq. (6). The electromagnetic field amplitudes, $F_\alpha(r,\theta,z)$, determined by the Hertz vectors Π_{jz}^σ can be written in the form of the Fourier integral as well with the Fourier-transformed amplitudes $\tilde{F}_\alpha(r,\theta;\beta)$ given in Appendix A. Now the Fourier-transformed Hertz vectors of the total reflected electromagnetic field can be written in the form

$$\tilde{\mathbf{\Pi}}_j^{(r)\sigma}=\tilde{\mathbf{\Pi}}_j^\sigma+\tilde{\Pi}_{jz}^\sigma\mathbf{e}_z. \tag{28}$$

The terms with different indices m in expansions (26) and (27) are linearly independent of each other. Therefore to satisfy boundary conditions for the total reflected electromagnetic field it is sufficient to consider only the terms with $m=n$. The continuity of the tangential field components at $r=a$ is reduced to the conditions imposed on the field Fourier-transformed amplitudes and can be written in a matrix form as follows:

$$\hat{M}(\beta)\vec{A}(\beta)=\vec{B}(\beta), \tag{29}$$

where

$$\hat{M}(\beta)=\begin{pmatrix} (\beta n/q_2^2 a)J_n(q_2a) & -(i\omega/cq_2)J_n'(q_2a) & -(\beta n/q_1^2 a)H_n^{(1)}(q_1a) & (i\omega/cq_1)H_n^{(1)\prime}(q_1a) \\ J_n(q_2a) & 0 & -H_n^{(1)}(q_1a) & 0 \\ (ik_2^2 c/\omega q_2)J_n'(q_2a) & (\beta n/q_2^2 a)J_n(q_2a) & -(ik_1^2 c/\omega q_1)H_n^{(1)\prime}(q_1a) & -(\beta n/q_1^2 a)H_n^{(1)}(q_1a) \\ 0 & J_n(q_2a) & 0 & -H_n^{(1)}(q_1a) \end{pmatrix}, \tag{30}$$

$$\vec{A}(\beta)=\begin{pmatrix} a_{2n}(\beta) \\ b_{2n}(\beta) \\ a_{1n}(\beta) \\ b_{1n}(\beta) \end{pmatrix}, \tag{31}$$

and

$$\vec{B}(\beta)=\begin{pmatrix} \Delta\tilde{E}_\theta(\beta) \\ \Delta\tilde{E}_z(\beta) \\ \Delta\tilde{H}_\theta(\beta) \\ \Delta\tilde{H}_z(\beta) \end{pmatrix}, \tag{32}$$

with $\Delta\tilde{E}_\alpha(\beta)\equiv\tilde{E}_{1\alpha}(a;\beta)-\tilde{E}_{2\alpha}(a;\beta)$ and $\Delta\tilde{H}_\alpha(\beta)\equiv\tilde{H}_{1\alpha}(a;\beta)-\tilde{H}_{2\alpha}(a;\beta)$; the quantities $\tilde{E}_{j\alpha}(r;\beta)$ and $\tilde{H}_{j\alpha}(r;\beta)$ are given in Appendix C. The solution of Eq. (29) is found as

$$A_k(\beta)=\frac{D_k(\beta)}{D(\beta)}, \tag{33}$$

where k numerates the components of the column $\vec{A}$, $D(\beta)\equiv\det\hat{M}(\beta)$, and D_k is the determinant of the matrix obtained from $\hat{M}$ by replacing its kth column with the column given by $\vec{B}$.

It is worthwhile to note that one can consider the Fourier representation of the electromagnetic field as a superposition of the plane waves $\exp(i\beta z)$. An integration over the real quantities β thus corresponds to the waves propagating toward both $z=-\infty$ and $z=+\infty$. To obtain a complete solution of the problem one has to consider β in the integrand of the Fourier integrals as a complex quantity and replace the integration along the real axis by that along a path of integration in the complex plane. This corresponds to taking into account the waves with complex propagation constants, i.e., those waves which describe transients in the vicinity of the nanofiber facet. To define the Fourier integral onto the complex plane of β it is necessary to analytically continue the Fourier-transformed quantities given by Eqs. (22), (26), and (27) to the values of q_j such that $-\pi<\mathrm{Arg}(q_j)\leq 0$. This can be done with the use of the relations

$$J_n(-\rho)=(-1)^n J_n(\rho), \tag{34}$$

$$H_n^{(1)}(-\rho)=(-1)^{n+1}H_n^{(2)}(\rho), \tag{35}$$

where $H_n^{(2)}$ is the Hankel function of the second kind. Let us note that formula (35) provides also an analytic continuation of Eq. (17) onto the whole complex plane of β.

As it follows from Eqs. (22), (26), and (27), the functions $\tilde{\mathbf{\Pi}}_j^{(r)\sigma}$ have branch points at $\beta=\pm k_j$ and to ensure a single-valued solution we make cuts on the complex plane of β drawn along the real axis from the branch points to $\pm\infty$. The functions $A_k(\beta)$ have poles given by the zeros of the denominator $D(\beta)$ which we denote as β_p. The real quantities β_p correspond to waveguide (bound) modes and they are disposed between k_1 and k_2, whereas those having an imaginary part $\mathrm{Im}(\beta_p)>0$ describe decaying modes (see Ref. 36 for the detail). As the determinant $D(\beta)$ is an even function of β, the quantities $-\beta_p$ are also the poles of $A_k(\beta)$. Figure 2 shows these poles along with the cuts and the accepted path of integration, C. The path C can be represented as a sum of the path embracing the left cut and running along its edges, and the one which runs along the lower edges of both cuts toward the positive direction of the real axis (not shown). The latter path can be closed by a semicircle of an infinite radius in the lower half-plane.[37] The obtained contour is reduced to a number of infinitesimal circles around the poles $-\beta_d$. The resulting contour C_- is also shown in Fig. 2. It completely lies in the left half-plane $\mathrm{Re}\,\beta<0$ and hence it corresponds to the waves reflected from the nanofiber facet. As a result, the Hertz vectors of the reflected field have the following form:

$$\mathbf{\Pi}_j^{(r)\sigma}=-\frac{i}{2}\sum_b \mathrm{Res}[\tilde{\Pi}_{jzu}^\sigma(-\beta_b)+\tilde{\Pi}_{jzl}^\sigma(-\beta_b)]e^{-i\beta_b z}\mathbf{e}_z - i\sum_d \mathrm{Res}[\tilde{\Pi}_{jz}^\sigma(-\beta_d)]e^{-i\beta_d z}\mathbf{e}_z+\mathbf{\Phi}_j^\sigma, \tag{36}$$

with

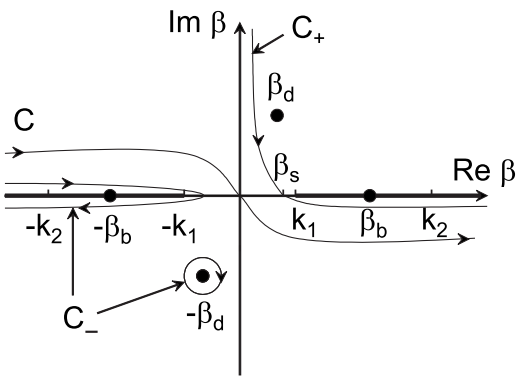

FIG. 2. Complex plane of β. The cuts and poles are shown by bold lines and dots, respectively. For simplicity, only a single waveguide mode and a single decaying mode are indicated. The integration paths C, C_- and C_+ are introduced in the text.

$$\mathbf{\Phi}_j^\sigma(z) = \frac{1}{2\pi} P \int_{-\infty}^{-k_1} \{[\tilde{\mathbf{\Pi}}_{ju}^\sigma(\beta) - \tilde{\mathbf{\Pi}}_{jl}^\sigma(\beta)] + [\tilde{\Pi}_{jzu}^\sigma(\beta) - \tilde{\Pi}_{jzl}^\sigma(\beta)]\mathbf{e}_z\} e^{i\beta z} d\beta, \tag{37}$$

where the symbol P in front of the integral means its principal value, $\mathrm{Res}[F(\beta)]$ is a residual of the function F at a point β, the subscripts u and l denote the values of the corresponding functions on the upper and lower edges of the cut, respectively, and the subscripts b and d numerate bound and decaying modes, respectively. The values of the functions on different edges of the cut are related to each other according to the following rules:[38]

$$F_u(\beta; q_1, q_2) = \begin{cases} F_l(\beta; -q_1, q_2) & \text{if } -k_2 < \beta < -k_1 \\ F_l(\beta; -q_1, -q_2) & \text{if } -\infty < \beta < -k_2, \end{cases} \tag{38}$$

and we accept that $\mathrm{Im}(q_1)$, $\mathrm{Im}(q_2) > 0$ on the lower edge of the cut.

Equation (36) gives an exact solution for the reflected electromagnetic field. It is interesting to consider this quantity at large distances from the nanowire end where the transient terms vanish. The term $\mathbf{\Phi}_j^\sigma$ in Eq. (36) can be estimated using integration by parts. In the leading order in $1/z$ one obtains

$$\mathbf{\Phi}_j^\sigma(z) \simeq \frac{1}{\pi z^2} \left[\left(\frac{d\tilde{\mathbf{\Pi}}_{ju}^\sigma}{d\beta} \right)_{\beta=-k_j} e^{-ik_j z} + \left(\frac{d\tilde{\Pi}_{jzu}^\sigma}{d\beta} \right)_{\beta=-k_1} e^{-ik_1 z} \mathbf{e}_z \right]. \tag{39}$$

Here, the first term in the brackets is the far-field limit for the radiation field created by the fictitious electric or magnetic surface currents located at $z=0$, whereas the second term originates from the fictitious currents at the outer nanowire surface. The terms in the second sum in Eq. (36) decay as $\exp[-|\mathrm{Im}(\beta_d)|z]$ and the sum over waveguide modes is dominant at large distances from the nanowire end.

In the limit $z \to -\infty$, the amplitude of the reflected wave has the only nonzero z component, $\psi_j^{(r)} \equiv \Pi_{jz}^{(r)e} + \Pi_{jz}^{(r)m}$, which can be written in the form

$$\psi_j^{(r)} = r_{00} \tilde{\psi}_j^{(i)} e^{-i\beta_{0z}} + \sum_{b \neq 0} (\tilde{\psi}_{jb}^e + \tilde{\psi}_{jb}^m) e^{-i\beta_{bz}}, \tag{40}$$

where $\tilde{\psi}_j^{(i)}$ and $\tilde{\psi}_{jb}^\sigma$ are defined by the equations

$$\psi_j^{(i)}(r,z) = \tilde{\psi}_j^{(i)}(r) e^{i\beta_{0z}}, \tag{41}$$

$$\tilde{\psi}_{jb}^\sigma(r) = -\frac{i}{2} \mathrm{Res}[\tilde{\Pi}_{jzu}^\sigma(r; -\beta_b) + \tilde{\Pi}_{jzl}^\sigma(r; -\beta_b)]. \tag{42}$$

All the Hertz vectors here depend on θ as $\exp(-in\theta)$ and this argument has been omitted for brevity. Equation (40) gives the backscattered wave with r_{00} the far-field reflection coefficient for the incident waveguide mode. This quantity does not depend neither on r nor on j and is reduced to the form

$$r_{00} = -\frac{i}{2} \{\mathrm{Res}[a_{2n}(-\beta_0; q_1) + a_{2n}(-\beta_0; -q_1) + b_{2n}(-\beta_0; q_1) + b_{2n}(-\beta_0; -q_1)]\}(a_{20} + b_{20})^{-1}. \tag{43}$$

The amplitudes $\tilde{\psi}_j^\sigma$ describe transformation of the incident wave into the other waveguide modes on reflection. It is reasonable to characterize its efficiency by the far-field transformation coefficient,

$$R_{0b} = -\frac{\int_0^{2\pi} \int_0^\infty \langle S_z^{(b)}(r,\theta) \rangle r dr d\theta}{\int_0^{2\pi} \int_0^\infty \langle S_z^{(i)}(r,\theta) \rangle r dr d\theta}, \tag{44}$$

where $\mathbf{S}^{(b)}$ and $\mathbf{S}^{(i)}$ are the Poynting vectors of the reflected bth waveguide mode and incident wave, respectively, and the angular brackets mean the time averaging.

IV. DIFFRACTION OF A WAVEGUIDE MODE

To calculate the electromagnetic field diffracted into surrounding medium one has to know the transmitted electric $\mathbf{E}''$ and magnetic $\mathbf{H}''$ fields in the plane $z=0$. These fields are found from Eqs. (9) and (10) where the reflected fields $\mathbf{E}'$ and $\mathbf{H}'$ originate from the Hertz vectors $\mathbf{\Pi}_j^{(r)e}$ and $\mathbf{\Pi}_j^{(r)m}$, Eq. (36). According to the Schelkunoff's formulation of the Equivalence Theorem,[34] the diffracted field can be found as it would be induced by the fictitious surface electric and magnetic current densities

$$\mathbf{L}^e = \frac{c}{4\pi} \mathbf{H}_t'' \tag{45}$$

and

$$\mathbf{L}^m = -\frac{c}{4\pi} \mathbf{E}_t'', \tag{46}$$

respectively, located in the plane $z=0$. The further consideration resembles that in Sec. II B where the current densities $\mathbf{K}^e$ and $\mathbf{K}^m$ must be replaced by $\mathbf{L}^e$ and $\mathbf{L}^m$, respectively. The Fourier-transformed amplitudes, $\tilde{\mathbf{\Pi}}_1^{(d)\sigma}(\beta)$, of the diffracted field Hertz vectors are given by Eq. (22) for $j=1$, where the vector functions $\mathbf{p}_\pm^\sigma(r)$ are replaced by $\mathbf{p}_\pm^\sigma(r) + \mathbf{q}_\pm^\sigma(r)$ with

$$\mathbf{q}_\pm^\sigma(r) = [\lambda_r^\sigma(r) \mp i\lambda_\theta^\sigma(r)](\mathbf{e}_r \pm i\mathbf{e}_\theta). \tag{47}$$

The quantities $\lambda_r^\sigma(r)$ and $\lambda_\theta^\sigma(r)$, which have been introduced here, are represented in Appendix D. Then the exact solution for the diffracted field, $\mathbf{\Pi}_1^{(d)\sigma}$, is given by the Fourier integral along the path of integration C_+ which lies completely in the right half-plane $\mathrm{Re}\,\beta > 0$.[39]

Let us consider this solution in the far zone, where not only $k_1\sqrt{r^2+z^2} \gg 1$ but also $q_1 r \gg 1$. In this limit, the quantity $\tilde{\mathbf{\Pi}}_1^{(d)\sigma}(\beta)$ is reduced to the form

$$\tilde{\mathbf{\Pi}}_1^{(d)\sigma}(r,\theta;\beta) \simeq \frac{i\pi^{3/2}}{\omega} \sqrt{\frac{2}{q_1 r}} e^{-i(2n+1)\pi/4} [\mathbf{S}_+^\sigma(\beta) - \mathbf{S}_-^\sigma(\beta)] e^{-in\theta} e^{iq_1 r}, \tag{48}$$

where

$$\mathbf{S}_{\pm}^{\sigma} = \frac{1}{\tau_\sigma}\int_0^\infty [\mathbf{p}_{\pm}^{\sigma}(r') + \mathbf{q}_{\pm}^{\sigma}(r')]J_{n\pm1}(q_1 r')r'dr'. \quad (49)$$

Introducing the angle of diffraction, χ, to the observation point $\mathbf{R}$ so that (see Fig. 1)

$$r = R\sin\chi, \quad z = R\cos\chi, \quad (50)$$

we consider $R=\sqrt{r^2+z^2}$ as a large parameter. Then the Fourier integral of $\tilde{\tilde{\mathbf{\Pi}}}_1^{(d)\sigma}(\beta)$ can be calculated with the use of the steepest descent method. Deforming the path C_+ so that it would run across the saddle point $\beta_s=k_1\cos\chi$ (Fig. 2), one obtains

$$\mathbf{\Pi}_1^{(d)\sigma}(R,\chi,\theta) \simeq \frac{i\pi}{\omega}e^{-i(2n+1)\pi/4}[\mathbf{S}_{+}^{\sigma}(\beta_s) - \mathbf{S}_{-}^{\sigma}(\beta_s)]\frac{e^{ik_1R}}{R}e^{-in\theta}. \quad (51)$$

Repeating this consideration for the field diffracted into the half-space $z<0$, one concludes that Eq. (51) is also valid in the far zone outside the nanowire.

From here one can calculate the electromagnetic field components in the far zone. In the leading order in $1/R$ the field is purely transversal ($E_R=H_R=0$) and the power diffracted within the elementary solid angle $d\Omega=\sin\chi d\chi d\theta$ is given by

$$dP(\chi) \simeq \frac{\pi\omega^2\epsilon_1^{3/2}}{8c^3}(|G_\chi(\chi)|^2 + |G_\theta(\chi)|^2)d\Omega, \quad (52)$$

where the functions

$$G_\chi(\chi) = \sqrt{\epsilon_1}(S_{-r}^{e} - S_{+r}^{e})\cos\chi - i(S_{-r}^{m} + S_{+r}^{m}) \quad (53)$$

and

$$G_\theta(\chi) = i\sqrt{\epsilon_1}(S_{-r}^{e} + S_{+r}^{e}) + (S_{-r}^{m} - S_{+r}^{m})\cos\chi \quad (54)$$

determine the χ dependence of the field components E_χ and E_θ, respectively, and all the quantities $S_{\pm r}^{\sigma}$ are taken at $\beta=\beta_s$. In the following, we shall characterize the angular distributions of the diffracted field polarized parallel to the vectors $\mathbf{e}_\mu$ ($\mu=\chi,\theta$) by the functions

$$\eta_\mu(\chi) = \frac{\pi\omega^2\epsilon_1^{3/2}}{8c^3}|G_\mu(\chi)|^2\left(\int_0^{2\pi}\int_0^\infty \langle S_z^{(i)}(r,\theta)\rangle r dr d\theta\right)^{-1}. \quad (55)$$

V. REFLECTION AND DIFFRACTION OF SYMMETRIC WAVEGUIDE MODES

The results obtained above are valid for arbitrary incident waveguide modes. They become, however, considerably simplified in the case of symmetric modes for which $n=0$. The Hertz vector of such modes is either transverse magnetic (e-type) or transverse electric (m-type). The determinant of the matrix $\hat{M}$, Eq. (30), is reduced to the form

$$D = D_{\mathrm{TM}}D_{\mathrm{TE}} \quad (56)$$

with

$$D_{\mathrm{TM}} = \frac{\omega}{c}\left[\frac{\epsilon_1}{q_1}J_0(q_2a)H_1^{(1)}(q_1a) - \frac{\epsilon_2}{q_2}J_1(q_2a)H_0^{(1)}(q_1a)\right] \quad (57)$$

and

$$D_{\mathrm{TE}} = \frac{\omega}{c}\left[\frac{1}{q_1}J_0(q_2a)H_1^{(1)}(q_1a) - \frac{1}{q_2}J_1(q_2a)H_0^{(1)}(q_1a)\right]. \quad (58)$$

The zeros of D_{TM} and D_{TE} with respect to β determine the propagation constants of TM and TE modes, respectively. Further we shall consider these two types of modes separately.

A. TM modes

In this case the incident wave is described by Eq. (8) with $b_{j0}=0$. Straightforward calculations with the use of equations given in Appendix C lead to the equality

$$\tilde{E}_{jr}(r;\beta) = \tilde{E}_{jz}(r;\beta) = \tilde{H}_{j\theta}(r;\beta) = 0. \quad (59)$$

As a result, the components of the column $\vec{A}(\beta)$, Eq. (31), have the form

$$a_{2n}(\beta) = a_{1n}(\beta) = 0, \quad (60)$$

$$b_{2n}(\beta) = \frac{2\pi^2}{\omega q_1}\frac{1}{D_{\mathrm{TE}}}\left\{\frac{2i}{\pi a}(k_1^2+\beta_0\beta)P_{1>}^{e}(a) + (k_2^2+\beta_0\beta)P_{2<}^{e}(a) \times[q_2H_1^{(1)}(q_1a)H_0^{(1)}(q_2a) - q_1H_0^{(1)}(q_1a)H_1^{(1)}(q_2a)]\right\}, \quad (61)$$

$$b_{1n}(\beta) = \frac{2\pi^2}{\omega q_2}\frac{1}{D_{\mathrm{TE}}}\left\{\frac{2i}{\pi a}(k_2^2+\beta_0\beta)P_{2<}^{e}(a) + (k_1^2+\beta_0\beta)P_{1>}^{e}(a) \times[q_2J_1(q_1a)J_0(q_2a) - q_1J_0(q_1a)J_1(q_2a)]\right\}. \quad (62)$$

Here the quantities $P_{1>}^{e}(a)$ and $P_{2<}^{e}(a)$ can be written explicitly as

$$P_{1>}^{e}(a) = \frac{\omega a_{10}}{4\pi q_{10}}I(H_1^{(1)},q_{10};H_1^{(1)},q_1), \quad (63)$$

$$P_{2<}^{e}(a) = -\frac{\omega a_{20}}{4\pi q_{20}}I(J_1,q_{20};J_1,q_2), \quad (64)$$

where the functions $I(Z^{(1)},p_1;Z^{(2)},p_2)$ are defined as

$$I(Z_1^{(1)},p;Z_1^{(2)},q) = \frac{a}{p^2-q^2}[pZ_2^{(1)}(pa)Z_1^{(2)}(qa) - qZ_1^{(1)}(pa)Z_2^{(2)}(qa)]. \quad (65)$$

Note that Eqs. (59) and (60) imply that the reflected field has a pure TE polarization. In other words, *the incident TM wave is not reflected—it is completely converted into a TE-polarized field on reflection*. This result can be understood as

follows. According to the equations of Appendix B, the incident wave induces the fictitious currents K_θ^e and K_r^m in the plane $z=0$. As it follows from the Biot-Savart law, the magnetic field associated with the current K_θ^e is parallel to the vector $\mathbf{e}_\theta \times \mathbf{R}$, where $\mathbf{R}$ is the radius-vector directed from the location of the elementary current to the observation point. One can formulate also an analog of the Biot-Savart law for a fictitious magnetic current K_r^m according to which the corresponding electric field should be parallel to the vector $\mathbf{e}_r \times \mathbf{R}$. This consideration leads to the same conclusions as Eqs. (59) and (60).

Let us assume that only a single pair of TM and TE waveguide modes exists at a given frequency ω. Then the incident TM wave can be converted into a single TE mode on reflection. In this case the transformation coefficient, Eq. (44), is found as

$$R_{01} = \frac{\beta_1}{4\beta_0} \frac{|\hat{b}_{2n}^+(-\beta_1) + \hat{b}_{2n}^-(-\beta_1)|^2}{|a_{20}|^2} \times \left(\frac{1}{q_{11}^2} - \frac{1}{q_{21}^2}\right) J_0(q_{21}a) J_2(q_{21}a) \left[\left(\frac{\epsilon_2}{q_{20}^2} - \frac{\epsilon_1}{q_{10}^2}\right) J_0^2(q_{20}a) - \frac{\epsilon_2(\epsilon_2 - \epsilon_1)}{\epsilon_1 q_{20}^2} J_1^2(q_{20}a) + \frac{2\epsilon_2}{q_{20}a}\left(\frac{1}{q_{10}^2} - \frac{1}{q_{20}^2}\right) J_0(q_{20}a) J_1(q_{20}a) \right]^{-1}, \tag{66}$$

where β_1 is the propagation constant of the TE mode, $q_{j1} = \sqrt{k_j^2 - \beta_1^2}$ and $\hat{b}_{2n}^{\pm}(\beta) = \mathrm{Res}[b_{2n}(\beta; \pm q_1)]$.

The functions $G_\chi(\chi)$ and $G_\theta(\chi)$, Eqs. (53) and (54), which determine the diffracted field have the form

$$G_\chi(\chi) = -2(1 + \cos^2\chi) \int_0^\infty \lambda_\theta^m(r') J_1(k_1 r' \sin\chi) r' dr', \tag{67}$$

$$G_\theta(\chi) = -\frac{i\omega\sqrt{\epsilon_1}}{2\pi} \left[\frac{a_{20}}{q_{20}} \left(\frac{\epsilon_2}{\epsilon_1} + \frac{\beta_0}{k_1}\cos\chi\right) \times I(J_1, q_{20}; J_1, k_1 \sin\chi) - \frac{a_{10}}{q_{10}} \left(1 + \frac{\beta_0}{k_1}\cos\chi\right) I(H_1^{(1)}, q_{10}; J_1, k_1 \sin\chi) \right]. \tag{68}$$

It follows from here that the quantity $G_\chi(\chi)$ is dictated by the reflected field, whereas the quantity $G_\theta(\chi)$ originates completely from the field of the incident wave. This means that these two contributions can be separated using an analyzer oriented parallel to either the vector $\mathbf{e}_\chi$ or the vector $\mathbf{e}_\theta$.

B. TE modes

In this case $a_{j0}=0$ and one obtains

$$\tilde{E}_{j\theta}(r;\beta) = \tilde{H}_{jr}(r;\beta) = \tilde{H}_{jz}(r;\beta) = 0. \tag{69}$$

The components of the column $\vec{A}(\beta)$, Eq. (31), are found as follows:

$$b_{2n}(\beta) = b_{1n}(\beta) = 0, \tag{70}$$

$$a_{2n}(\beta) = \frac{2i\pi^2}{c\beta_0 q_1} \frac{1}{D_{\mathrm{TM}}} \left\{ \frac{2i\epsilon_1}{\pi a}(k_1^2 + \beta_0\beta) P_{1>}^e(a) - (k_2^2 + \beta_0\beta) P_{2<}^e(a) [\epsilon_1 q_2 H_1^{(1)}(q_1 a) H_0^{(1)}(q_2 a) - \epsilon_2 q_1 H_0^{(1)}(q_1 a) H_1^{(1)}(q_2 a)] \right\}, \tag{71}$$

$$a_{1n}(\beta) = -\frac{2i\pi^2}{c\beta_0 q_2} \frac{1}{D_{\mathrm{TM}}} \left\{ \frac{2i\epsilon_2}{\pi a}(k_2^2 + \beta_0\beta) P_{2<}^e(a) + (k_1^2 + \beta_0\beta) P_{1>}^e(a) [\epsilon_1 q_2 J_1(q_1 a) J_0(q_2 a) - \epsilon_2 q_1 J_0(q_1 a) J_1(q_2 a)] \right\}, \tag{72}$$

where the quantities $P_{1>}^e(a)$ and $P_{2<}^e(a)$ are given by

$$P_{1>}^e(a) = -\frac{ic\beta_0 b_{10}}{4\pi\epsilon_1 q_{10}} I(H_1^{(1)}, q_{10}; H_1^{(1)}, q_1), \tag{73}$$

$$P_{2<}^e(a) = \frac{ic\beta_0 b_{20}}{4\pi\epsilon_2 q_{20}} I(J_1, q_{20}; J_1, q_2). \tag{74}$$

As one can conclude from Eqs. (69) and (70), *the incident TE wave is completely converted into a TM-polarized field on reflection*. As it has been discussed above, this can be understood on the basis of the Biot-Savart law. The corresponding transformation coefficient, Eq. (44), in the case where only a single pair of symmetric modes exists has the form

$$R_{01} = \frac{\beta_1}{4\beta_0} \frac{|\hat{a}_{2n}^+(-\beta_1) + \hat{a}_{2n}^-(-\beta_1)|^2}{|b_{20}|^2} \times \left[\left(\frac{1}{q_{10}^2} - \frac{1}{q_{20}^2}\right) J_0(q_{20}a) J_2(q_{20}a) \right]^{-1} \times \left[\left(\frac{\epsilon_2}{q_{21}^2} - \frac{\epsilon_1}{q_{11}^2}\right) J_0^2(q_{21}a) - \frac{\epsilon_2(\epsilon_2 - \epsilon_1)}{\epsilon_1 q_{21}^2} J_1^2(q_{21}a) + \frac{2\epsilon_2}{q_{21}a}\left(\frac{1}{q_{11}^2} - \frac{1}{q_{21}^2}\right) J_0(q_{21}a) J_1(q_{21}a) \right], \tag{75}$$

where now β_1 is the propagation constant of the TM mode and $\hat{a}_{2n}^{\pm}(\beta) = \mathrm{Res}[a_{2n}(\beta; \pm q_1)]$.

For the angular distributions of the diffracted field one obtains

$$G_\chi(\chi) = \frac{i\omega}{2\pi} \left(1 + \frac{\beta_0}{k_1}\cos\chi\right) \left[\frac{b_{20}}{q_{20}} I(J_1, q_{20}; J_1, k_1 \sin\chi) - \frac{b_{10}}{q_{10}} I(H_1^{(1)}, q_{10}; J_1, k_1 \sin\chi) \right], \tag{76}$$

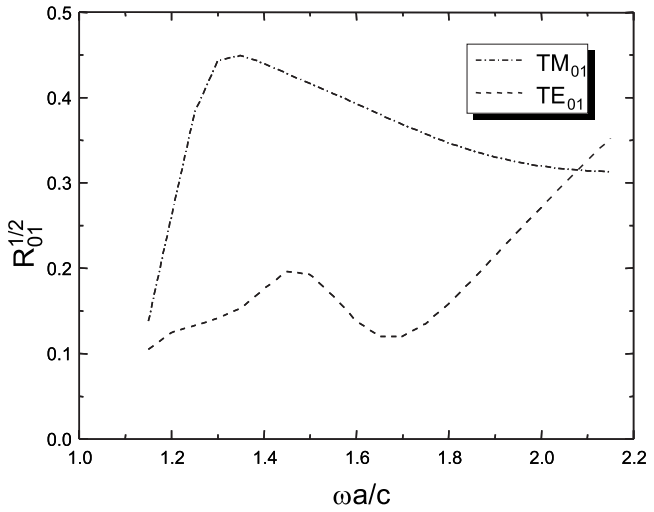

FIG. 3. Frequency dependence of the transformation coefficient. The polarization of the incident waveguide mode is indicated in the inset. $\epsilon_1=1$, $\epsilon_2=6$.

$$G_\theta(\chi)=2\int_0^\infty\left[\frac{\lambda_\theta^e(r')}{\sqrt{\epsilon_1}}-\lambda_r^m(r')\cos\chi\right]J_1(k_1r'\sin\chi)r'dr'. \tag{77}$$

Here the quantity $G_\chi(\chi)$ is determined by the incident wave field, whereas the quantity $G_\theta(\chi)$ originates from the reflected field.

C. Numerical results

We shall illustrate the results obtained above for symmetric waveguide modes by some numerical examples. To compare our calculations with those carried out using the finite-difference time-domain method[24,25] we take the dielectric constant of the nanowire $\epsilon_2=6$ and $\epsilon_1=1$ for surrounding medium. The far-field reflection coefficient, Eq. (43), is identically equal to zero for both TM and TE incident waveguide modes. Figure 3 represents the far-field transformation coefficient $\sqrt{R_{01}}$, which can be compared with the "reflection coefficient" calculated in Ref. 24 It has been plotted in the frequency range where only a single pair of symmetric modes exists. The magnitude of this quantity is approximately the same as in Fig. 4 of Ref. 24 but its frequency dependence and the ratio $R_{01}^{\mathrm{TM}}/R_{01}^{\mathrm{TE}}$ are different. A direct comparison, however, is not possible because that paper deals with evolution of a wave packet which propagates along a nanowire of finite length. As a result, the reflected field contains, besides the far-field contribution determined by Eq. (40), the near-field components originating from the slowly decreasing term $\mathbf{\Phi}_j^\sigma(z)$, Eq. (37), and the decaying modes. Let us note that due to the nonstationary character of the problem the modes decaying both in the z-coordinate and in time contribute to the reflected field (see Ref. 36).

Figure 4 shows the quantities η_μ, Eq. (55), as a function of the diffraction angle. Both dependencies display a pronounced peak at some angle χ_m. As for symmetric modes the field is invariant relative to the rotations around the nanowire axis, the peak in the χ dependence means that the maximum diffracted field intensity forms a cone with the angular opening $2\chi_m$. The position of this maximum differs for different modes which allows one to determine which mode is excited in the nanowire. Note that there is no emitted intensity along the nanowire axis where $\chi\simeq 0$. This conclusion as well as the positions of the diffracted field maxima is in agreement with the results obtained in Ref. 25.

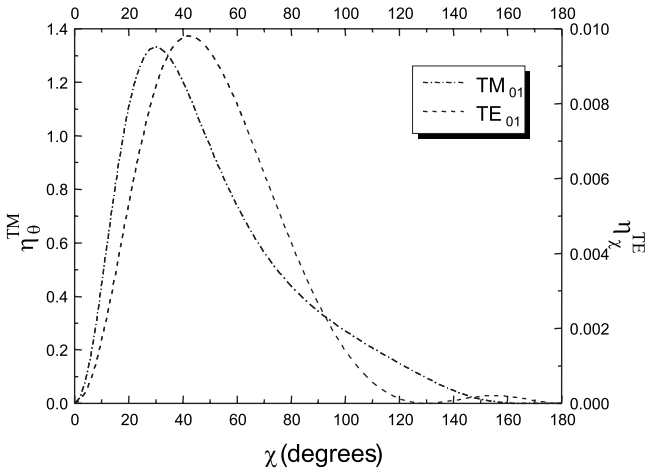

FIG. 4. Angular dependence of the diffracted field intensity calculated for $\omega a/c=1.5$, $\epsilon_1=1$, $\epsilon_2=6$. The polarization of the incident waveguide mode is indicated in the inset.

VI. CONCLUSION

In this paper, we have found an exact rigorous solution for the problem of diffraction at the end of a dielectric cylindrical nanowire. The solution has the form of the Fourier integral along a path of integration in the complex plane of propagation constants. Deforming this path, one obtains either the field reflected from the nanowire end or the diffracted field. The general solution has been analyzed in detail for the case of symmetric waveguide modes. A remarkable feature of this case is a complete conversion of the incident TM-polarized mode into a TE-polarized mode on reflection, and vice versa. The corresponding diffracted field intensity forms a cone the angular opening of which is specific for a given waveguide mode. The diffracted fields originating from the incident mode and reflected mode can be separated by an appropriate orientation of an analyzer.

It is worthwhile to note that the knowledge of the diffracted field of a definite waveguide mode allows one to find, using the relations of reciprocity,[40] the amplitude of such a mode excited in the waveguide by an incident plane wave.

The obtained results allow one to treat also the case of a nanowire of finite length. If at such a length the transient terms in the field reflected from one nanowire facet can be neglected, this field has the form of a superposition of waveguide modes incident at the other nanowire facet. In particular, if an incident wave is a symmetric waveguide mode it is converted in itself after double reflection at different facets. This implies that TM and TE modes in the nanowire will propagate in the opposite directions. The corresponding re-

flection coefficient can be calculated using the equations of Secs. V A and V B. The Fabry-Pérot symmetric modes in such a resonator will be dictated by its length as well as by the phase of the reflection coefficient.

APPENDIX A: FIELD AMPLITUDES

The field amplitudes dictated by the Hertz vectors $\Pi_{jz}^{\sigma}\mathbf{e}_z$ are obtained by their substitution in Eqs. (1) and (2). The result has the form of the Fourier integrals with the Fourier-transformed quantities given by the following equations (the argument $q_j r$ of the cylindrical functions has been omitted for brevity):

$$\tilde{E}_{jr} = \sum_{m=-\infty}^{\infty} \left(\frac{i\beta}{q_j} Z'_m a_{jm} + \frac{\omega m}{c q_j^2 r} Z_m b_{jm} \right) e^{-im\theta}, \tag{A1}$$

$$\tilde{E}_{j\theta} = \sum_{m=-\infty}^{\infty} \left(\frac{\beta m}{q_j^2 r} Z_m a_{jm} - \frac{i\omega}{c q_j} Z'_m b_{jm} \right) e^{-im\theta}, \tag{A2}$$

$$\tilde{E}_{jz} = \sum_{m=-\infty}^{\infty} Z_m a_{jm} e^{-im\theta}, \tag{A3}$$

$$\tilde{H}_{jr} = \sum_{m=-\infty}^{\infty} \left(-\frac{c k_j^2 m}{\omega q_j^2 r} Z_m a_{jm} + \frac{i\beta}{q_j} Z'_m b_{jm} \right) e^{-im\theta}, \tag{A4}$$

$$\tilde{H}_{j\theta} = \sum_{m=-\infty}^{\infty} \left(\frac{i c k_j^2}{\omega q_j} Z'_m a_{jm} + \frac{\beta m}{q_j^2 r} Z_m b_{jm} \right) e^{-im\theta}, \tag{A5}$$

$$\tilde{H}_{jz} = \sum_{m=-\infty}^{\infty} Z_m b_{jm} e^{-im\theta}. \tag{A6}$$

The field amplitudes of the incident wave, Eq. (8), can be written as

$$F_{\alpha}^{(i)}(r,\theta,z) = \tilde{F}_{\alpha}^{(i)}(r,\theta) e^{i\beta_0 z}, \tag{A7}$$

where the quantities $\tilde{F}_{\alpha}^{(i)}$ can be formally obtained from the above equations if one takes a single term with $m=n$ and uses the substitutions

$$\beta \to \beta_0, \quad q_j \to q_{j0}, \quad a_{jn} \to a_{j0}, \quad b_{jn} \to b_{j0}. \tag{A8}$$

APPENDIX B: FICTITIOUS CURRENT COMPONENTS κ_{μ}^{σ}

The components κ_r^{σ} and κ_{θ}^{σ} which determine the fictitious currents, Eq. (20), are found as follows:

$$\kappa_r^e(r) = \frac{c}{4\pi} \left[-\frac{c k_j^2 n}{\omega q_{j0}^2 r} Z_n(q_{j0} r) a_{j0} + \frac{i\beta_0}{q_{j0}} Z'_n(q_{j0} r) b_{j0} \right], \tag{B1}$$

$$\kappa_{\theta}^e(r) = \frac{c}{4\pi} \left[\frac{i c k_j^2}{\omega q_{j0}} Z'_n(q_{j0} r) a_{j0} + \frac{\beta_0 n}{q_{j0}^2 r} Z_n(q_{j0} r) b_{j0} \right], \tag{B2}$$

$$\kappa_r^m(r) = -\frac{c}{4\pi} \left[\frac{i\beta_0}{q_{j0}} Z'_n(q_{j0} r) a_{j0} + \frac{\omega n}{c q_{j0}^2 r} Z_n(q_{j0} r) b_{j0} \right], \tag{B3}$$

$$\kappa_{\theta}^m(r) = -\frac{c}{4\pi} \left[\frac{\beta_0 n}{q_{j0}^2 r} Z_n(q_{j0} r) a_{j0} - \frac{i\omega}{c q_{j0}} Z'_n(q_{j0} r) b_{j0} \right]. \tag{B4}$$

APPENDIX C: FICTITIOUS FIELD AMPLITUDES

The amplitudes of the electromagnetic field induced by the fictitious currents in the half-space $z<0$ can be obtained by inserting the Hertz vectors [Eq. (21)] into Eqs. (1) and (2). Their Fourier-transformed components have the form

$$\tilde{F}_{j\alpha}(\theta;\beta) = \tilde{F}_{j\alpha}(\beta) e^{-in\theta}, \tag{C1}$$

where the quantities $\tilde{F}_{j\alpha}(\beta)$ are given by the equations

$$\begin{aligned} \tilde{E}_{jr}(r;\beta) = -\frac{\pi^2}{\omega} \Bigg[& \beta \left(\beta P_{j<}^e - i\frac{\omega}{c} P_{j<}^m \right) H_{n-1}^{(1)}(q_j r) \\ & + \beta \left(\beta P_{j>}^e - i\frac{\omega}{c} P_{j>}^m \right) J_{n-1}(q_j r) \\ & + \beta \left(\beta Q_{j<}^e + i\frac{\omega}{c} Q_{j<}^m \right) H_{n+1}^{(1)}(q_j r) \\ & + \beta \left(\beta Q_{j>}^e + i\frac{\omega}{c} Q_{j>}^m \right) J_{n+1}(q_j r) \\ & + \frac{n q_j}{r} (P_{j<}^e + Q_{j<}^e) H_n^{(1)}(q_j r) \\ & + \frac{n q_j}{r} (P_{j>}^e + Q_{j>}^e) J_n(q_j r) + \frac{2i}{\pi \tau_e} (p_{-r}^e + p_{+r}^e) \Bigg], \end{aligned} \tag{C2}$$

$$\begin{aligned} \tilde{E}_{j\theta}(r;\beta) = \frac{\pi^2}{\omega} \Bigg[& \left(i k_j^2 P_{j<}^e + \beta \frac{\omega}{c} P_{j<}^m \right) H_{n-1}^{(1)}(q_j r) \\ & + \left(i k_j^2 P_{j>}^e + \beta \frac{\omega}{c} P_{j>}^m \right) J_{n-1}(q_j r) \\ & - \left(i k_j^2 Q_{j<}^e - \beta \frac{\omega}{c} Q_{j<}^m \right) H_{n+1}^{(1)}(q_j r) \\ & - \left(i k_j^2 Q_{j>}^e - \beta \frac{\omega}{c} Q_{j>}^m \right) J_{n+1}(q_j r) \\ & - i\frac{n q_j}{r} (P_{j<}^e - Q_{j<}^e) H_n^{(1)}(q_j r) \\ & - i\frac{n q_j}{r} (P_{j>}^e - Q_{j>}^e) J_n(q_j r) \Bigg], \end{aligned} \tag{C3}$$

$$\tilde{E}_{jz}(r;\beta) = \frac{\pi^2}{\omega} q_j \left\{ \left[i\beta(P^e_{j<} - Q^e_{j<}) + \frac{\omega}{c}(P^m_{j<} + Q^m_{j<}) \right] H^{(1)}_n(q_j r) + \left[i\beta(P^e_{j>} - Q^e_{j>}) + \frac{\omega}{c}(P^m_{j>} + Q^m_{j>}) \right] J_n(q_j r) \right\}. \tag{C4}$$

Here the following functions have been introduced:

$$P^\sigma_{j<}(r) = \frac{1}{\tau_\sigma} \int_{L_{j<}} p^\sigma_{-r}(r') J_{n-1}(q_j r') r' dr', \tag{C5}$$

$$P^\sigma_{j>}(r) = \frac{1}{\tau_\sigma} \int_{L_{j>}} p^\sigma_{-r}(r') H^{(1)}_{n-1}(q_j r') r' dr', \tag{C6}$$

$$Q^\sigma_{j<}(r) = \frac{1}{\tau_\sigma} \int_{L_{j<}} p^\sigma_{+r}(r') J_{n+1}(q_j r') r' dr', \tag{C7}$$

$$Q^\sigma_{j>}(r) = \frac{1}{\tau_\sigma} \int_{L_{j>}} p^\sigma_{+r}(r') H^{(1)}_{n+1}(q_j r') r' dr', \tag{C8}$$

with the intervals of integration defined as

$$L_{j<} = \begin{cases} [a,r] & \text{if } j=1 \\ [0,r] & \text{if } j=2, \end{cases} \tag{C9}$$

and

$$L_{j>} = \begin{cases} [r,\infty) & \text{if } j=1 \\ [r,a] & \text{if } j=2. \end{cases} \tag{C10}$$

The amplitudes $\tilde{H}_{jr}$, $\tilde{H}_{j\theta}$ and $\tilde{H}_{jz}$ can be formally obtained from $\tilde{E}_{jr}$, $\tilde{E}_{j\theta}$ and $\tilde{E}_{jz}$, respectively, using the substitutions

$$P^e_{j\alpha} \to P^m_{j\alpha}, \quad Q^e_{j\alpha} \to Q^m_{j\alpha},$$

$$P^m_{j\alpha} \to -\epsilon_j P^e_{j\alpha}, \quad Q^m_{j\alpha} \to -\epsilon_j Q^e_{j\alpha},$$

$$\tau_e \to \tau_m, \quad p^e_{\pm r} \to p^m_{\pm r}, \tag{C11}$$

where the subscript α acquires the values $\langle$or$\rangle$. Note that

$$P^\sigma_{1<}(a) = Q^\sigma_{1<}(a) = P^\sigma_{2>}(a) = Q^\sigma_{2>}(a) = 0. \tag{C12}$$

APPENDIX D: FICTITIOUS CURRENT COMPONENTS λ^σ_μ

The fictitious currents components at $z=+0$ are determined by the reflected field. Deforming the path of integration C_- so that it would run along the imaginary axis in the β-plane one obtains

$$\lambda^e_r(r) = -\frac{c}{4\pi} \int_{-i\infty}^{i\infty} \left[\tilde{H}_{jr}(r;\beta) - \frac{ck_j^2 n}{\omega q_j^2 r} Z_n(q_j r) a_{jn}(\beta) + \frac{i\beta}{q_j} Z'_n(q_j r) b_{jn}(\beta) \right] d\beta, \tag{D1}$$

$$\lambda^e_\theta(r) = -\frac{c}{4\pi} \int_{-i\infty}^{i\infty} \left[\tilde{H}_{j\theta}(r;\beta) + \frac{ick_j^2}{\omega q_j} Z'_n(q_j r) a_{jn}(\beta) + \frac{\beta n}{q_j^2 r} Z_n(q_j r) b_{jn}(\beta) \right] d\beta, \tag{D2}$$

$$\lambda^m_r(r) = \frac{c}{4\pi} \int_{-i\infty}^{i\infty} \left[\tilde{E}_{jr}(r;\beta) + \frac{i\beta}{q_j} Z'_n(q_j r) a_{jn}(\beta) + \frac{\omega n}{c q_j^2 r} Z_n(q_j r) b_{jn}(\beta) d\beta \right], \tag{D3}$$

$$\lambda^m_\theta(r) = \frac{c}{4\pi} \int_{-i\infty}^{i\infty} \left[\tilde{E}_{j\theta}(r;\beta) + \frac{\beta n}{q_j^2 r} Z_n(q_j r) a_{jn}(\beta) - \frac{i\omega}{c q_j} Z'_n(q_j r) b_{jn}(\beta) \right] d\beta, \tag{D4}$$

where the quantities $\tilde{E}_{jr}$, $\tilde{E}_{j\theta}$, $\tilde{H}_{jr}$, and $\tilde{H}_{j\theta}$ are given in Appendix C and the coefficients a_{jn} and b_{jn} are determined by Eqs. (31) and (33). Here the integrands do not have poles along the chosen path of integration.

*bordo@mci.sdu.dk

[1] X. Duan, Y. Huang, Y. Cui, J. Wang, and C. M. Lieber, Nature (London) **409**, 66 (2001).
[2] J. Wang, M. S. Gudiksen, X. Duan, Y. Cui, and C. M. Lieber, Science **293**, 1455 (2001).
[3] M. H. Huang, S. Mao, H. Feick, H. Yan, Y. Wu, H. Kind, E. Weber, R. Russo, and P. Yang, Science **292**, 1897 (2001).
[4] J. C. Johnson, H.-J. Choi, K. P. Knutsen, R. D. Schaller, P. Yang, and R. J. Saykally, Nat. Mater. **1**, 106 (2002).
[5] X. Duan, Y. Huang, R. Agarwal, and C. M. Lieber, Nature (London) **421**, 241 (2003).
[6] F. Balzer and H.-G. Rubahn, Adv. Funct. Mater. **15**, 17 (2005).
[7] F. Balzer and H.-G. Rubahn, Appl. Phys. Lett. **79**, 3860 (2001).
[8] M. Schiek, A. Lützen, R. Koch, K. Al-Shamery, F. Balzer, R. Frese, and H.-G. Rubahn, Appl. Phys. Lett. **86**, 153107 (2005).
[9] L. Tong, R. R. Gattass, J. B. Ashcom, S. He, J. Lou, M. Shen, I. Maxwell, and E. Mazur, Nature (London) **426**, 816 (2003).
[10] F. Balzer, V. G. Bordo, A. C. Simonsen, and H.-G. Rubahn, Phys. Rev. B **67**, 115408 (2003).
[11] J. C. Johnson, H. Yan, P. Yang, and R. J. Saykally, J. Phys. Chem. **107**, 8816 (2003).
[12] C. J. Barrelet, A. B. Greytak, and C. M. Lieber, Nano Lett. **4**, 1981 (2004).
[13] K. Thilsing-Hansen, M. T. Neves-Petersen, S. B. Petersen, R. Neuendorf, K. Al-Shamery, and H.-G. Rubahn, Phys. Rev. B **72**, 115213 (2005).
[14] R. Agarwal, C. J. Barrelet, and C. M. Lieber, Nano Lett. **5**, 917 (2005).

[15] F. Quochi, F. Cordella, A. Mura, G. Bongiovanni, F. Balzer, and H.-G. Rubahn, J. Phys. Chem. **109**, 21690 (2005).
[16] F. Quochi, F. Cordella, A. Mura, G. Bongiovanni, F. Balzer, and H.-G. Rubahn, Appl. Phys. Lett. **88**, 041106 (2006).
[17] V. Volkov, S. I. Bozhevolnyi, V. G. Bordo, and H.-G. Rubahn, J. Microsc. **215**, 241 (2004).
[18] J. Brewer, C. Maibohm, L. Jozefowski, L. Bagatolli, and H.-G. Rubahn, Nanotechnology **16**, 2396 (2005).
[19] J. Brewer and H.-G. Rubahn, Phys. Status Solidi C **2**, 4058 (2005).
[20] J. Fiutowski, V. G. Bordo, L. Jozefowski, M. Madsen, and H.-G. Rubahn, Appl. Phys. Lett. **92**, 073302 (2008).
[21] Y. Nakayama, P. J. Pauzauskie, A. Radenovic, R. M. Onorato, R. J. Saykally, J. Liphardt, and P. Yang, Nature (London) **447**, 1098 (2007).
[22] H. C. van de Hulst, *Light Scattering by Small Particles* (Wiley, New York, 1957).
[23] V. G. Bordo, Phys. Rev. B **73**, 205117 (2006).
[24] A. V. Maslov and C. Z. Ning, Appl. Phys. Lett. **83**, 1237 (2003).
[25] A. V. Maslov and C. Z. Ning, Opt. Lett. **29**, 572 (2004).
[26] C. J. Bouwkamp, Rep. Prog. Phys. **17**, 35 (1954).
[27] L. A. Vajnshtejn, *Teoriya Diffraktzii i Metod Faktorizatzii* (Sovetskoe Radio, Moskva, 1966) (in Russian); See also H. Hönl, A. W. Maue, and K. Westpfahl, *Theorie der Beugung* (Springer-Verlag, Berlin, 1961).
[28] S. Asano and G. Yamamoto, Appl. Opt. **14**, 29 (1975); See also, C. F. Bohren and D. R. Huffman, *Absorption and Scattering of Light by Small Particles* (Wiley, New York, 1983).
[29] F. González and F. Moreno, in *Light Scattering from Microstructures*, Lecture Notes in Physics Vol. 534, edited by F. González and F. Moreno (Springer-Verlag, Berlin, 2000).
[30] S. Bruzzone, M. Malvaldi, G. P. Arrighini, and C. Guidotti, J. Phys. Chem. B **109**, 3807 (2005).
[31] L. Novotny and B. Hecht, *Principles of Nano-Optics* (Cambridge University Press, Cambridge, England, 2006).
[32] J. A. Stratton, *Electromagnetic Theory* (McGraw-Hill, New York, 1941).
[33] Here and in the following we omit the factor $\exp(-i\omega t)$ for brevity. Note that even and odd waves for which the θ-dependence is given by $\cos(n\theta)$ and $\sin(n\theta)$, respectively, can be considered as a superposition of two waves with amplitudes proportional to $e^{-in\theta}$ and $e^{in\theta}$.
[34] S. A. Schelkunoff, Phys. Rev. **56**, 308 (1939).
[35] I. S. Gradshteyn and I. M. Ryzhik, *Table of Integrals, Series and Products* (Academic, New York, 1994).
[36] V. G. Bordo, J. Phys.: Condens. Matter **19**, 236220 (2007).
[37] One can show that the Fourier-transformed amplitudes given by Eq. (28) tend to zero when $|\beta| \to \infty$. Then, according to the Jordan's lemma, the integral about the semicircle is equal to zero if $z < 0$.
[38] The quantity $q_j^2 = k_j^2 - \beta^2$ changes its sign twice when one moves from one edge of the cut to another around the branch point. This means that its argument acquires a shift of 2π. Correspondingly, the quantity q_j acquires a factor $\exp(i\pi) = -1$.
[39] The validity of such a deformation of the integration path C can be proved in much the same way as it was done for the path C_- in Sec. III.
[40] M. L. Levin, Dokl. Akad. Nauk SSSR **60**, 787 (1948) (in Russian).